ANNALS OF GEOPHYSICS, 66, 5, RS529, 2023; doi: 10.4401/ag-9009
OPEN ACCESS

Point clouds repeatability and fast scale factor estimates in free SfM surveying: terrestrial application and empirical approach

Arianna Pesci[*,1], Giordano Teza[2], Fabiana Loddo[1]

(1) Istituto Nazionale di Geofisica e Vulcanologia, Sezione di Bologna, Bologna, Italy
(2) Alma Mater Studiorum University of Bologna, Department of Physics and Astronomy "A. Righi", Bologna, Italy

Article history: received September 6, 2023; accepted December 21, 2023

Abstract

Previous experiments highlighted the possible existence of a relation between repeatability of point clouds obtained from Structure-from-Motion photogrammetry (SfM), represented by the standard deviation (σ), and the nominal ground sampling distance (GSD). In particular, the empirical relation $3\sigma \sim 2.5\ GSD$ was found. For this reason, in-situ tests aimed at studying this relation were carried out. Data from seven surveys carried out in 2018-2022 time span allowed the comparison between 20 pairs of almost contemporary point clouds, generated by means of relative bundle adjustment (BA) without ground control points (GCPs) and then relatively scaled and aligned. In this way, the relation $3\sigma = aGSD$ was found, where $a = 2.5 \pm 0.4$. This result also suggested the use of the reverse procedure, where the scale factor (SF) is estimated from the standard deviation of non-metric point clouds, σ_{nmu}, by using the relation $SF_a = aGSD/3\sigma_{nmu}$. Additional checks proved that SF_a differs from SF by 3%. This error is not acceptable error for length, area or volume measurements, but the estimated SF_a is more than adequate for a fast, rough registration of photogrammetric models aimed at searching patterns or precursors of incipient phenomena in impervious/inaccessible areas or in emergency conditions.

Keywords: SfM; Relative bundle adjustment; Scale factor; Uncertainty modeling

1. Introduction

Structure from Motion (SfM) is a photogrammetric technique largely used in geological/geomorphological surveying [see e.g. Brunier et al. 2016] as well as in civil engineering/architectural surveying [see e.g. Mistretta et al., 2019]. This is because a photorealistic point cloud or also a 3D model can be easily obtained thanks to very efficient algorithms for fully or quasi-completely automatic alignment and images processing. The equipment for SfM surveying is nothing more than a digital camera, even prosumer, and simple accessories (e.g. tripods or stabilizers). A good result in terms of photorealistic models depends on the quality of taken images, the coverage/oversampling of the observed area and the algorithms efficiency. Nowadays, Open Source software featuring performances similar to those of commercial software packages such as Metashape is also available [Cutugno et al., 2022].

Indirect georeferencing (IG) or direct georeferencing (DG) allow the creation of metric and georeferenced point clouds, 3D/2.5D models, orthoimages, etc. In particular, IG runs using several ground control point (GCPs) acquired with topographical techniques (e.g. GNSS survey, total station) and detectable in some images. The GCP coordinates are useful in the Bundle Block Adjustment (BBA), providing a georeferenced point cloud as the photogrammetric modeling is completed [see e.g. Eltner et al., 2016]. An adequate distribution of GCPs in the observed area is essential, especially for large areas acquisition [Martínez-Carricondo, et al., 2018; Yan et al., 2017].

The DG is typically used in aerial SfM and replaces GCPs with GNSS-assisted BBA. The camera position at each shot is measured by means of an integrated GNSS receiver coupled with an inertial navigation unit and connected to a base station within Real Time Kinematic (RTK) approach, as shown e.g. by [Zhang et al., 2019]. Here, the requirement is a centimeter GCP accuracy [Salas Lopez et al., 2022].

Despite the availability of RTK equipped professional or prosumer cameras, in case of emergency or areas inaccessibility or very hard problems in GCPs installation and measuring, when a fast and safe surveying is an essential requirement, a relative bundle adjustment (BA) should run without constraints, i.e. without accurate ground coordinates. Point clouds resulting from a very automatic images analysis, without external measurements, are non-metric and non-aligned into a reference frame. Therefore, a scale factor is necessary. Moreover, in a completely free approach, the propagation of errors on images alignment could lead to point cloud distortions as instrumental drift effects [Sanz-Ablanedo et al., 2018]. The procedure aimed at fixing the problem consists in the generation of a series of point clouds to represent parts of the observed whole surface and the alignment of them to build a complete model, but is extremely time consuming.

Scaling a non-metric point cloud with the polyline-method [Pesci et al., 2016] is an easy and efficient operation, based on selecting easily recognizable points in the point cloud and measuring the length of the closed polyline that connects them. The ratio between the lengths of this polyline and of the corresponding one defined in a metric reference frame provides the scale factor.

Experiments based on artificial targets and in situ multitemporal surveys, carried out without IG and DG in the Central Apennine area in Italy, led to establish that the resolution limit (R_L) is linked to the Ground Sampling Distance (GSD) by the empirical relation $R_L \sim 2.5\ GSD$ [Pesci et al., 2020]. This study also included an evaluation of the effects of acquisition settings, in particular observation geometry and focal length, on the quality of the final photogrammetric model. However, some systematisms appeared because of a very oblique rock cliff and consequent significant deformation of pixels on the ground. Because of this evidence, a new experiment focusing on the point cloud precision was performed in order to understand whether geometry was the problem [Pesci et al., 2019]. A subvertical cliff was observed in normal incidence and with different focal lengths. No significant systematic effects were observed and, moreover, the empirical relation $3\sigma \sim 2.5\ GSD$, where σ is the standard deviation (SD) of the distribution of differences, was obtained.

The aim of this new work is to confirm the validity in a wide range of cases of the relation $3\sigma = aGSD$, where a is a parameter to be estimated, and to discuss its potential for a raw estimation of the scale factor.

2. Test site, measurements and data processing

The surveyed surface is a rock cliff inside the "Riserva Naturale Contrafforte Pliocenico" (Bologna province, Emilia Romagna region, Northern Italy). The latter consists of a 15 km long complex formed by rocky outcrops of Pliocene sandstone [Ente di gestione per i Parchi e la Biodiversità, 2023]. It is transversal to the valleys of some rivers and torrents (Setta, Savena, Zena, and Idice) and extends from Sasso Marconi to Monte delle Formiche. The Contrafforte Pliocenico rocks are due to sedimentation of sands and gravels carried by Apennine torrents within a wide marine gulf in the Pliocene (52 Ma ago) which corresponds to large part of the current Appennino Bolognese. The cliff hosts a natural rock-climbing gym, is sub-vertical and about 100 m high with respect the road below. It is ideal for terrestrial photogrammetry experiments thanks to the very good views and acquisition points spacing (Figure 1), but cliff sub-verticality makes it hard GCPs placing and measuring. A first study on the application of SfM to this specific test site is shown in [Pesci et al., 2019], where the aim was the search of possible systematic effects in case of view in normal incidence and for different focal lengths.

Seven measurement campaigns were carried out in the 2018-2022 time span acquiring the cliff from a mean distance of 340 m. For each survey, an operator walked (round trip) for about 400 m along a road parallel to the rock wall (Figure 1) taking images by means of a Nikon D3300 camera with the criterion of a high overlap

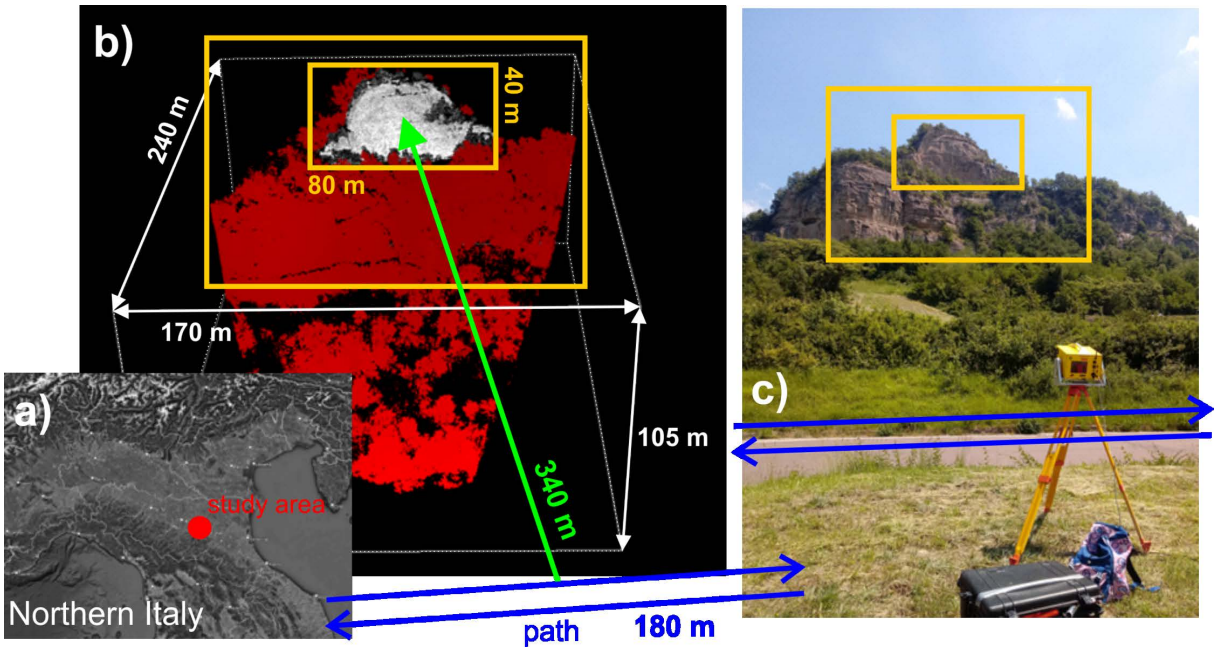

Figure 1. Test area: (a) localization; (b) TLS point cloud with some measured distances; (c) view of the cliff. The walking direction (round trip) for data acquisition is also shown (blue arrows).

between the images, i.e. 80-100% depending on the used focal length f (55 mm ≤ f ≤ 200 mm were considered in these experiments). The shorter the f, the wider the field, which has an impact on image overlap. But, the shorter the f, the greater the GSD with obvious repercussions on the accuracy of the final model. If a short f is used, the observed object can be captured integrally in all images with 100% overlap, preventing possible alignment systematisms.

For each measurement epoch and focal length, subsequent surveys were carried out in similar light conditions with similar camera positions and orientations along the walking path by taking a first set of images forward and the second returning, leading to two independent sets of images for subsequent processing carried out by using Metashape package. In order to carry out the photogrammetric modeling, some options about alignment, point cloud quality and filtering are selected. Some tests with different options were used to establish recommended choices. These main results were obtained:

- Image alignment: the better solution is “high accuracy”, i.e. full-size images. The tests with “highest accuracy” (upscaling by a factor 2 for each side, and therefore by a global factor 4) did not provide good results; besides a calculation time more than quadrupled, the result worsened. The option “medium accuracy” (downscaling by a factor 4) could be suitable in particular conditions (e.g. inadequate light conditions or excessive vegetation cover), but the results could generally be improved. Finally, “lower accuracy” (downscaling by a factor 16) is not recommended in these applications;
- Point cloud generation: the better solution is “high quality”, i.e. the images are subsampled by a factor 4 (2 for each side). Despite a quadrupling of the calculation time, the results obtained in terms of precision, i.e. repeatability, did not vary if “ultrahigh quality” (full-size images) was chosen instead of “high quality” (note the “asymmetry” in the Metashape terms: in the alignment stage “high” means full-size, whereas in the photogrammetric stage “high” corresponds to a subsampling by a factor 4). This result should be related to the strong oversampling that characterize the photogrammetric surveys; each point of the scene must be acquired from at least two different positions, in fact many more, to have good photogrammetric modeling. On the contrary, for lower quality levels the repeatability could be unstable and, therefore, cannot be used for analysis of precision;
- Depth filtering: good and similar results were obtained with “mild” and “moderate” filtering. Disabling depth filtering led to point clouds characterized by strong noise, and therefore unsuitable for repeatability analysis. On the contrary, “aggressive filtering” led to point clouds excessively smoothed, also in this case unsuitable for repeatability analysis.

Since the typical performance of a currently available desktop/laptop equipped with CUDA (Compute Unified Device Architecture) GPU (Graphics Processing Unit) allows extensive photogrammetric calculations also in emergency conditions, the recommended solutions are: high accuracy image alignment, high quality modeling, and moderate (or also mild) depth filtering.

A reference terrestrial laser scanning (TLS) survey performed in 2019 from the same mean distance with about 2 cm sampling step allowed the generation of a metric point cloud with ~10^6 points with radiometric information in near infrared band (wavelength $\lambda = 1535$ nm). The TLS point cloud provided the constraints for SfM models scaling using the polyline method [Pesci et al., 2016]. Some common points or details (e.g. stones, architectural elements, dihedral corners) well visible in all point clouds and well distributed all along the studied area allowed the creation of a closed polyline and the computation of its length in each point cloud. A good point distribution is very important to warrant a stable reference for the whole surface. The ratio between each polyline length and the reference one is the relative scale factor. If the reference polyline comes from a metric point cloud (as the TLS point cloud is), the ratios are the reliable scale factors. The Innovmetric PolyWorks software package was used for point and polyline selection and measurements.

Table 1 summarizes: acquisition dates, focal lengths, numbers of images used for the data processing and analysis (N_A) and numbers of images used for next verifications (N_T), GSDs at 340 m, which is the reference distance (*GSD*), later on simply called reference GSD, polyline lengths (*L*), relative scale factors (SF_R) and absolute scale factors (*SF*), i.e. scale factors obtained by using the TLS-based point cloud. The application of the polyline method in this specific case, is shown in Figure 2. Four points framing a large portion of the surface inside the polyline (connecting them) are chosen in each point cloud.

Date	*f* (mm)	N_A	N_T	*GSD* (m)	*L* (nmu)[1]	SF_R (%)	*SF* (%)
28/03/2018	55	33	—	0.024	2.04385	112.68	4611.39
28/03/2018	55	35	—	0.024	2.16051	106.60	4362.40
28/03/2018	98	33	—	0.014	11.76706	19.57	800.96
28/03/2018	98	35	—	0.014	2.81403	81.84	3349.29
03/06/2021	55	20	20	0.024	1.60626	143.38	5867.66
03/06/2021	55	22	20	0.024	1.56906	146.78	6006.76
03/06/2021	100	19	20	0.013	2.80061	82.23	3365.34
03/06/2021	100	17	18	0.013	1.98053	116.28	4758.83
03/06/2021	200	43	38	0.007	2.06232	111.67	4570.10
03/06/2021	200	34	38	0.007	4.00150	57.55	2355.37
23/09/2021	55	25	24	0.024	8.62562	26.70	1092.68
23/09/2021	55	20	23	0.024	8.05531	28.59	1170.04
23/09/2021	70	20	20	0.019	1.90222	121.07	4954.75
23/09/2021	70	18	19	0.019	1.66426	138.38	5663.17
23/09/2021	85	19	18	0.016	1.85034	124.47	5093.67

[1] nmu states for non-metric unit

Date	f (mm)	N_A	N_T	GSD (m)	L (nmu)[1]	SF_R (%)	SF (%)
23/09/2021	85	17	17	0.016	1.27302	180.91	7403.64
23/09/2021	110	21	20	0.012	2.17614	105.83	4331.07
23/09/2021	110	18	17	0.012	1.98455	116.05	4749.18
26/04/2022	55	28	24	0.024	1.72376	133.60	5467.70
26/04/2022	55	26	26	0.024	10.16483	22.66	927.22
26/04/2022	70	23	24	0.019	5.93845	38.78	1587.11
26/04/2022	70	26	24	0.019	2.10415	109.45	4479.24
26/04/2022	98	23	24	0.014	1.96598	117.14	4794.05
26/04/2022	98	23	22	0.014	1.96582	117.15	4794.44
26/04/2022	120	25	24	0.011	7.02324	32.79	1341.97
26/04/2022	120	24	24	0.011	2.11023	109.14	4466.34
17/05/2022	55	42	40	0.024	10.35600	22.24	910.10
17/05/2022	55	44	38	0.024	2.29629	100.29	4104.45
17/05/2022	116	46	40	0.011	2.29999	100.13	4097.84
17/05/2022	116	44	40	0.011	2.87425	80.13	3279.12
01/06/2022	55	35	33	0.024	16.80393	13.71	560.88
01/06/2022	55	36	33	0.024	1.98028	116.30	4759.42
01/06/2022	116	37	35	0.011	2.38860	96.42	3945.83
01/06/2022	116	37	34	0.011	14.35012	16.05	656.79
20/09/2022	55	31	30	0.024	2.20663	104.37	4271.21
20/09/2022	55	32	30	0.024	2.35481	97.80	4002.44
20/09/2022	105	35	32	0.013	2.76975	83.15	3402.84
20/09/2022	105	35	32	0.013	2.66373	86.46	3538.27
20/09/2022	**155**	**31**	**30**	**0.009**	**2.30303**	**100.00**	**4092.44**
20/09/2022	155	31	28	0.009	1.71723	134.11	5488.49

[1] nmu states for non-metric unit

Table 1. Main data about surveys and corresponding scale factors. The reference point cloud used for relative scaling is highlighted in bold.

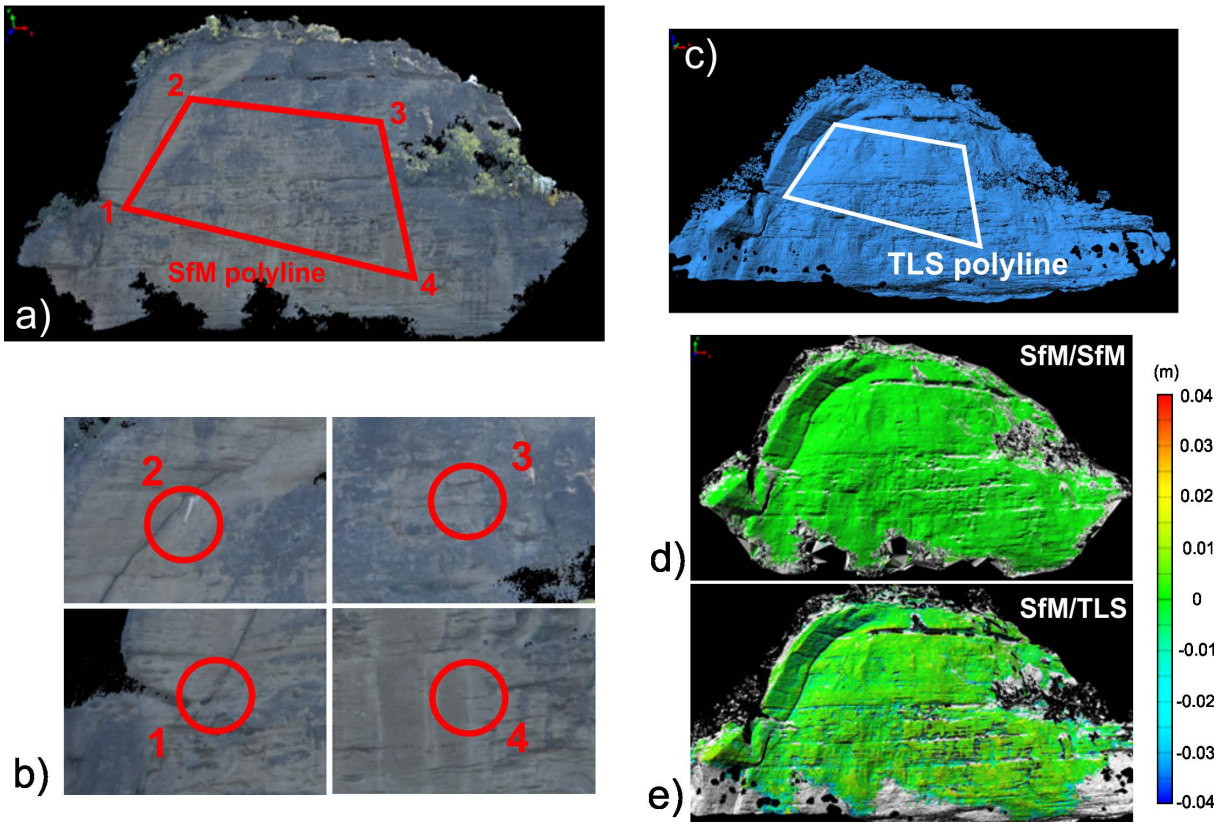

Figure 2. Polyline method: (a) polyline selected in a SfM point cloud; (b) recognized features (circle centers); (c) reference polyline, whose length is 94.25 m; (d) example of map of differences between two co-scaled, metric SfM point clouds; (e) example of map of differences between a metric SfM point cloud and the reference, TLS-based one. Data from images acquired in May 2022 ($f = 116$ mm).

Actually, the value of the polyline length comes from the average of ten repetitions to eliminate/mitigate any systematic errors. The same approach applies to the length of the reference TLS polyline. Moreover, in order to also evaluate the results of scaling with respect to a same non-metric point cloud, and therefore simulate a case where non-metric data are available, relative scale factors SF_R where also computed. In this case, the SfM point cloud generated with data taken in September 2022 survey with $f = 155$ mm focal length (bold row in Table 1) is used as the reference. In Fig. 2 the comparison between a metric SfM point cloud and the TLS one is also shown, putting on evidence a quite good spatial and dimensional agreement. The errors are smaller than the expected resolution limits and no systematic effects lie outside the areas characterized by disturbance due to vegetation cover.

The comparison of contemporary point clouds pairs, characterized by the same camera settings (and, therefore, the same GSD), is based on point clouds alignment and subsequent generation of differences maps.

Since the measurement campaigns carried out in 2018 had different purposes, there are no additional photos for a first SF estimation and subsequent test in this case. For this reason, two independent subsets of images were obtained by means of random mixing of available images. The resulting point clouds, as in the case of 2021 and 2022 data, allowed the calculation of the differences and corresponding SD (σ). Table 2 summarizes, for all the considered cases, focal lengths, GSDs, SDs and $3\sigma/GSD$ ratios. It seems that there exists an empirical relation:

$$3\sigma = aGSD, \tag{1}$$

where $a = 2.5 \pm 0.4$ and

$$GSD = pd/f, \tag{2}$$

where in turn p is the sensor pixel size (3.9 µm in the case of Nikon D3300), d is the acquisition distance (340 m in this case) and f is the focal length. It is interesting to note that this result is similar to the one obtained in [Pesci et al., 2020] and related to the resolution, i.e.

$$R_L = bGSD, \tag{3}$$

where R_L is the resolution limit, namely the smaller element visible and measurable in a point cloud and $b = 2.3 \pm 0.5$. The result is not obvious, even if the two quantities considered are somehow correlated since they both come from the same photogrammetric modeling; if a terminology borrowed from radar interferometry is used, σ is mainly inherent to the range, while R_L is mainly related to the cross-range.

Date	f (mm)	GSD (m)	σ (m)	$a = \frac{3\sigma}{GSD}$
28/03/2018	55	0.024	0.021	2.6
28/03/2018	98	0.014	0.011	2.4
03/06/2021	55	0.024	0.020	2.5
03/06/2021	100	0.013	0.011	2.5
03/06/2021	200	0.007	0.006	2.6
23/09/2021	55	0.024	0.021	2.6
23/09/2021	70	0.019	0.016	2.5
23/09/2021	85	0.016	0.014	2.6
23/09/2021	110	0.012	0.011	2.8
26/04/2022	55	0.024	0.018	2.3
26/04/2022	70	0.019	0.016	2.5
26/04/2022	98	0.014	0.012	2.6
26/04/2022	120	0.011	0.009	2.5
17/05/2022	55	0.024	0.021	2.6
17/05/2022	116	0.011	0.009	2.5
01/06/2022	55	0.024	0.018	2.3
01/06/2022	116	0.011	0.010	2.7
20/09/2022	55	0.024	0.020	2.5
20/09/2022	105	0.013	0.011	2.5
20/09/2022	155	0.009	0.007	2.3
			Average a:	2.5 ± 0.4

Table 2. Standard deviations, GSDs and their ratios.

3. A possible use of the empirical relation

Equation (1) suggests a method that could provide a preliminary estimate of the scale factor starting from point clouds generated by means of a relative BA approach and without metrical constraints as reference metric models, GCPs or DG. The estimate of the scale factor to obtain metric objects based on the a parameter, from now on indicated with the symbol SF_a, is

$$SF_a = aGSD/(3\sigma_{nmu}) \tag{4}$$

where σ_{nmu} is the SD of the distribution of differences between a pair of relatively scaled non-metric point clouds. If this relation is true and stable, then it could be used to compute a scale factor from the original unscaled point clouds. However, it is important to evaluate what is the difference between SF_a and the true SF. At this point the additional data for the tests (column N_T in Table 1) come into play, to verify the results with independent data sets. The comparison of the new pairs of point clouds, co-scaled and co-registered in the non-metric system, provides the differences, the SDs and the SF_a estimates by imposing the parameter 2.5. Table 3 shows the results and the global ratio $SF_a/SF = 99.7\% \pm 2.5\%$. The corresponding relative difference $(SF_a - SF)/SF$ never exceeds 3%. The scale factor, therefore, can be calculated from the raw data and independently within the limit of a 3% error. The procedure needs two point clouds, indicatively each with 50% of the total acquired images, to run, and an estimate of the rough mean camera-object distance to provide the GSD. The estimate SF_a provides a preliminary and rough scaling, useful for very fast applications and for the study of possible patterns and deformations.

Date	f (mm)	GSD (m)	σ_{nmu} (nmu)	SF_a/SF (%)
28/03/2018	55	0.024	0.00096	97.74
28/03/2018	98	0.014	0.00280	102.97
03/06/2021	55	0.024	0.00034	100.00
03/06/2021	100	0.013	0.00037	98.66
03/06/2021	200	0.007	0.00027	98.65
23/09/2021	55	0.024	0.00500	98.17
23/09/2021	70	0.019	0.00032	98.96
23/09/2021	85	0.016	0.00083	98.42
23/09/2021	110	0.012	0.00090	97.43
26/04/2022	55	0.024	0.00300	101.22
26/04/2022	70	0.019	0.00101	98.96
26/04/2022	98	0.014	0.00025	97.22
26/04/2022	120	0.011	0.00067	101.85
17/05/2022	55	0.024	0.00550	98.00
17/05/2022	116	0.011	0.00022	101.85
01/06/2022	55	0.024	0.01500	102.38

Date	f (mm)	GSD (m)	σ_{nmu} (nmu)	SF_a/SF (%)
01/06/2022	116	0.011	0.00090	97.65
20/09/2022	55	0.024	0.00047	100.00
20/09/2022	105	0.013	0.00032	98.48
20/09/2022	155	0.009	0.00050	102.44
			Averaged SF_a/SF (%)	99.7 ± 2.5

Table 3. Differences between estimated (SF_a) and true (SF) scale factors.

4. Discussion and conclusions

In a previous work aimed at investigating possible systematisms in point clouds obtained from long range terrestrial SfM, a relation between SDs of distribution of differences between contemporaneous point clouds and GSD was found [Pesci et al., 2019]. This empirical relation, Eq. (1), was very similar to the one between resolution limit and GSD, obtained both in experiments with artificial targets and in situ tests, therefore in different observation conditions, Eq.(3) [Pesci et al., 2020]. The present work is aimed at confirming, or excluding, this empirical relation. The data from about 40 SfM point clouds obtained from the images taken by means of a Nikon D3300 prosumer camera in seven measurement campaigns from 2018 to 2022 confirmed the relation, expressed in Eq. (1), where $a = 2.5 \pm 0.4$. Some measurements were also carried out by means of a Nikon D750 full-frame camera, leading to $a = 2.4 \pm 0.2$ for f =120 mm, $a = 2.6 \pm 0.3$ for f =110 mm and $a = 2.5 \pm 0.3$ for f =55 mm. Although the measurements with the full frame camera were numerically limited and not systematic as in the case of the tests with the prosumer one, it is reasonable to hypothesize that the empirical parameter a could be representative for a large amount of applications with different devices under the condition that at least prosumer cameras with ~1.5 crop factor are used. If a poor-quality camera with a crop factor of 3 or 4 is used instead, a different empirical relation is expected because there are some issues related to both the real GSD and the photogrammetric modeling. For example, systematisms in photogrammetric models can be observed if drones with compact, low quality cameras are used [Pesci et al., 2018; Pesci et al, 2022].

Since the obtained result, relating SD and GSD, suggested a way to provide a first estimate of the scale factor, as shown by Eq. (4), other image datasets acquired during the measurement sessions were used to verify this hypothesis. The results show that the difference between the scale factor estimated in this quick and approximate way, SF_a, and the true SF, obtained from metric data, never exceed 3%. The implications of up to 3% error for the scaling factor are significant for the quality of the information obtained from the SF_a-scaled SfM point clouds. Fig. 3 shows the results of the comparison between the point clouds. In particular, the difference maps between two SfM point clouds related to the April 2022 (f =70 mm) survey and scaled with SF and SF_a are shown in Fig. 3.a and 3.b respectively. There is a good agreement. Systematism are not present as well as significant differences except for vegetated areas. The difference maps between the used SfM point cloud and the TLS point cloud are shown in Figure 3c (SF-scaled SfM point cloud) and Figure 3d (SF_a-scaled SfM point cloud). In the SF-scaled case there is total agreement, while in the SF_a-scaled case there are significant discrepancies. On the one hand, this means that 3% scale error is not adequate if the aim is to measure lengths, surfaces or volumes. On the other hand, if the aim is the search for patterns and precursors (i.e. small variations one or more orders of magnitude smaller than the size of the surveyed area), the SF_a estimated in this way can provide acceptable results. In emergency conditions, it may be essential not so much to have precise measurements of occurred variations, but to recognize that some variations really occurred and provide a first, rough estimate of them. This can be very useful in several contexts, for example: search for traces of detachment or trails of falling/rolling rock on a cliff; changes in the discontinuity surfaces of a stratified rock with subvertical or in any case very inclined layers which could lead to toppling; soil swelling in volcanic environment; deformations due to earthquake-induced soil liquefaction; variations in

inclination of milestones or other recognizable features; in general, topographic changes. Clearly, the monitored phenomenon must be compatible with the precision of a rough estimate. For example, a landslide in which decimeter displacements (even localized) occurred in the time between two surveys can be easily studied, but a rock landslide with millimeter displacements or displacements limited to a few centimeters cannot be studied in this way, except in the case in which there are localized features.

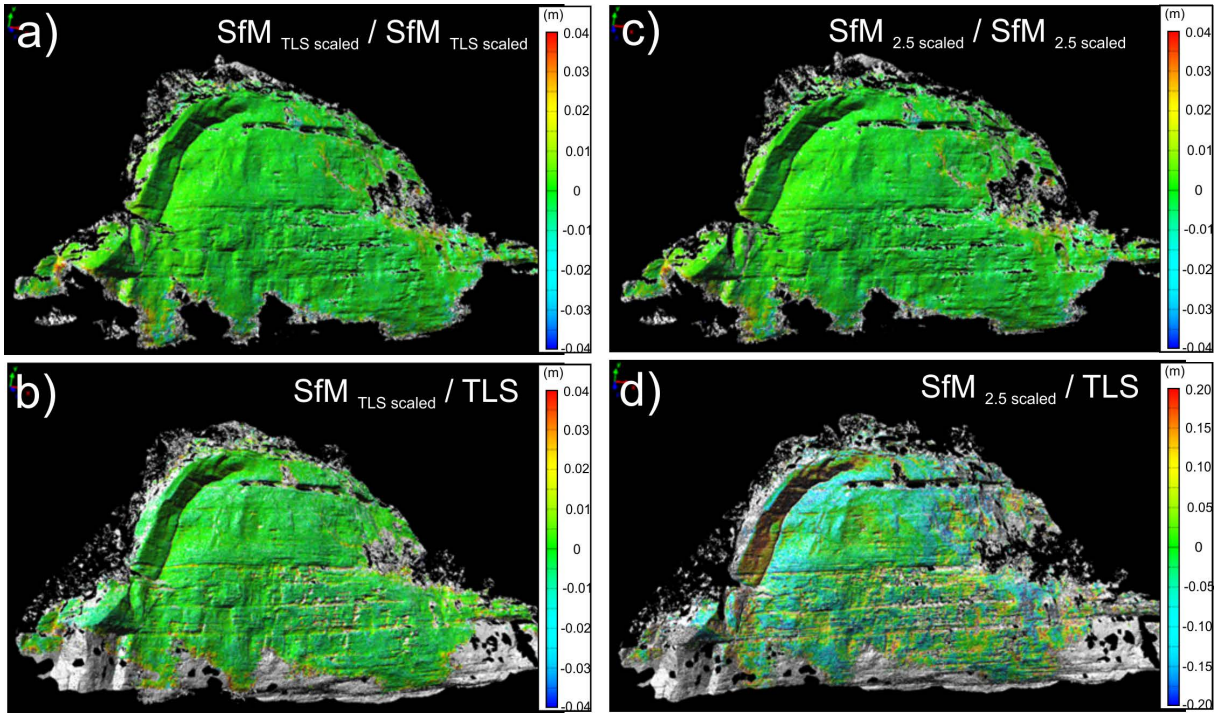

Figure 3. Maps of differences between point clouds: (a) *SF*-scaled SfM point clouds, range from –0.04 to 0.04 m; (b) SF_a-scaled SfM point clouds, range from –0.04 to 0.04 m; (c) *SF*-scaled SfM point cloud with respect to the TLS one, range from –0.04 to 0.04 m; (d) SF_a-scaled SfM point cloud with respect to the TLS one, range from –0.25 to 0.25 m.

The proposed method for quick SF estimation aimed at obtaining almost metric results despite the lack of targets, GCPs or GNSS-based camera positioning systems. In this way, it is possible to have qualitative and quantitative information even in case of emergency conditions, prohibitive logistics, inaccessibility, or also scarce availability of economic resources. Only the mean camera-target distance is a need as external measure, but it can be easily obtainable using a cheap portable laser rangefinder or other free and available data. A previous study [Pesci et al., 2020] also showed that the baselines extracted from Google Earth (GE) allowed to obtain a scale factor with an error of about 3%, therefore comparable with the proposed method. Although GE data are widely available worldwide, in the case of terrestrial surveys in mountain areas or in areas where there are strong topographic gradients the precision of the measurements and, above all, the ability to find homologous points, strongly deteriorate. A scale factor estimated with GE data for a sub-vertical cliff could have a uncertainty significantly greater than the SF_a estimated with Eq. (4).

The SF_a estimation is affected by various sources of errors, including the reference distance estimation, the calculation of GSD based on general geometric criteria, the different lighting conditions throughout measurement campaigns, the different number of images for each survey and so on. It is important to underline again that, as above stated, Eq. (4) provides reasonable estimates only provided that at least a prosumer camera with ~1.5 crop factor is used.

An operational recommendation is to initially scale the multitemporal point clouds together, taking advantage of the presence of similar RGB features, and only at a later time apply the SF correction and therefore switch from a common non-metric to a metric reference frame.

The use of TLS in this study does not contradict the aim of finding a fast, independent and low-cost method for the free detection of SfM; on the contrary, it is a very safe way to evaluate well the limits of a SF estimated in this way by means of empirical relations.

In conclusion, the proposed method for the quick SF estimation in absence of reliable metrical data has proven to be capable to provide results affected by errors of a few percent; these errors are incompatible with the accurate measure of lengths, surfaces or volumes but are good enough for the search of patterns, which is among the main objectives of surveying natural or artificial surfaces. Future research will allow to test the limit size of a system below which it is reasonable to use the relative BA and, therefore, to scale the point clouds using the proposed approach.

Data availability statement. The images captured during the measurement campaigns are available for further analysis or interest in reprocessing.

Acknowledgments. The authors wish to thank INGV for funding this research within the institutional project "Ricerca Libera 2019".

References

Brunier, G., J. Fleury, J.E. Anthony, V. Pothin, C. Vella, P. Dussouillez, A. Gardel and E. Michaud (2016). Structure-from-Motion photogrammetry for high-resolution coastal and fluvial geomorphic surveys, Géomorphologie, 22, 2, 147-161. https://doi.org/10.1007/978-3-319-58304-4_9.

Cutugno, M., U. Robustelli and G. Pugliano (2022). Structure-from-Motion 3D Reconstruction of the Historical Overpass Ponte della Cerra: A Comparison between MicMac® Open Source Software and Metashape®, Drones, 6, 9, 242, https://doi.org/10.3390/drones6090242.

Eltner, A, A. Kaiser, C. Castillo, G. Rock, F. Neugirg and A. Abellán (2016). Image-based surface reconstruction in geomorphometry-merits, limits and developments, Earth Surf. Dyn., 4, 2, 359-389, https://doi.org/10.5194/esurf-4-359-2016.

Ente di gestione per i Parchi e la Biodiversità (2023). Contrafforte Pliocenico Nature Reserve web page. Available online at: https://enteparchi.bo.it/en/contrafforte-pliocenico-nature-reserve/ (accessed: November 23, 2023).

Martínez-Carricondo, P., F. Agüera-Vega, F. Carvajal-Ramírez, F.-J. Mesas-Carrascosa, A. García-Ferrer and F.-J. Pérez-Porras (2018). Assessment of UAV-photogrammetric mapping accuracy based on variation of ground control points, Int. J. Appl. Earth Obs. Geoinf., 72, 1-10, https://doi.org/10.1016/j.jag.2018.05.015.

Mistretta, F., G. Sanna, F. Stochino and G. Vacca (2019). Structure from Motion Point Clouds for Structural Monitoring, Remote Sens., 11, 1940, https://doi.org/10.3390/rs11161940.

Pesci, A., G. Teza, M. Bisson, F. Muccini, P. Stefanelli, M. Anzidei, R. Carluccio, I. Nicolosi, A. Galvani, V. Sepe and C. Carmisciano (2016). A fast method for monitoring the coast through independent photogrammetric measurements: application and case study, J. Geosci. Geomat., 4, 4, 73-81. https://doi.og/10.12691/jgg-4-4-1.

Pesci, A., V. Kastelic, G. Teza, M. Carafa, P. Burrato and R. Basili (2018). Utilizzo della fotogrammetria SfM terrestre per il monitoraggio dei versanti: considerazioni sulle precisioni per applicazioni a lunga distanza, Rapporto tecnico INGV, 394, 1-20.

Pesci, A., G. Teza and F. Loddo (2019). Low cost Structure-from-Motion-based fast surveying of a rock cliff: precision and reliability assessment, Quad. Geofis., INGV, 156, 1-22. https://doi.org/10.13127/qdg/156.

Pesci, A., G. Teza, V. Kastelic and M.M.C. Carafa (2020). Resolution and precision of fast, long range terrestrial photogrammetric surveying aimed at detecting slope changes, J. Surv. Eng., 146, 4, 04020017-1-13. https://doi.org/10.1061/(ASCE)SU.1943-5428.0000328.

Pesci, A., G. Teza, F. Loddo, M. Fabris, M. Monego and S. Amoroso (2022). Studio di possibili effetti sistematici nelle nuvole di punti SfM da APR: confronti con TLS, distorsioni e metodi di mitigazione/Evaluation of possible systematic effects in SfM UAV based point clouds: TLS and surface variations for error mitigation methods, Quad. Geofis., INGV, 177, 1-22, https://doi.org/10.13127/qdg/177.

Salas López, R., R.E. Terrones Murga, J.O. Silva-López, N.B. Rojas-Briceño, D. Gómez Fernández, M. Oliva-Cruz and Y. Taddia (2022). Accuracy Assessment of Direct Georeferencing for Photogrammetric Applications Based on UAS-GNSS for High Andean Urban Environments, Drones, 6, 12, 388, https://doi.org/10.3390/drones6120388.

Sanz-Ablanedo, E., J.H. Chandler, J.R. Rodríguez-Pérez and C. Ordóñez (2018). Accuracy of Unmanned Aerial Vehicle (UAV) and SfM Photogrammetry Survey as a Function of the Number and Location of Ground Control Points Used, Remote Sens., 10, 10, 1606, https://doi.org/10.3390/rs10101606.

Yan, L., R. Chen, H. Sun, Y. Sun, L. Liu and Q. Wang (2017). A novel bundle adjustment method with additional ground control point constraint, Remote Sen. Lett., 8, 1, 68-77, https://doi.org/10.1080/2150704X.2016.1235809.

Zhang, H., E. Aldana-Jague, F. Clapuyt, F. Wilken, V. Vanacker and K. Van Oost (2019). Evaluating the potential of post-processing kinematic (PPK) georeferencing for UAV-based structure- from-motion (SfM) photogrammetry and surface change detection, Earth Surf. Dyn., 7, 807-827, https://doi.org/10.5194/esurf-7-807-2019.

***CORRESPONDING AUTHOR: Arianna PESCI**,
Istituto Nazionale di Geofisica e Vulcanologia, Sezione di Bologna,
Bologna, Italy
e-mail: arianna.pesci@ingv.it